International Journal of Science and Qualitative Analysis
2015; 1(3): 54-63
Published online August 6, 2015 (http://www.sciencepublishinggroup.com/j/ijsqa)
doi: 10.11648/j.ijsqa.20150103.13

Modeling of Bio-inspired Thunnus Albacares and Inchworm-gammarus with Micro Actuators in One Structure

A. Shourangiz Haghighi[1, *], I. Zare[2], Mohammad Ahmadi Balootaki[3], Mohammad Orak[3], Omid Zare[4]

[1]Department of Mechanical Engineering, Jahrom University, Jahrom, Iran
[2]Department of Cell and Molecular Biology, Semnan University, Semnan, Iran
[3]Department of Mechanical Engineering, Najaf Abad Branch, Islamic Azad University, Isfahan, Iran
[4]Department of Electrical Power Technology Engineering, Shahid Chamran Kerman University of Technology, Kerman, Iran

Email address:

A. shourangizhaghighi.2015@ieee.org (A. S. Haghighi), I_Zare@aol.com (I. Zare), Mohammad_ahmadi@smc.iaun.ac.ir (M. A. Balootaki), Mohammad_orak@smc.iaun.ac.ir (M. Orak), O.Zare.elec@gmail.com (O. Zare)

To cite this article:

A. Shourangiz Haghighi, I. Zare. Mohammad Ahmadi Balootaki, Mohammad Orak, Omid Zare. Modeling of Bio-inspired Thunnus Albacares and Inchworm-gammarus with Micro Actuators in One Structure. *International Journal of Science and Qualitative Analysis*. Vol. 1, No. 3, 2015, pp. 54-63. doi: 10.11648/j.ijsqa.20150103.13

Abstract: Biomimetic robots have attracted many researches around the world and also living creatures are the best models in biomimetic robotic engineering design. This paper is the combination of three creatures such as tuna, inchworm, gammarus. They are used in order for shortcoming of unrealized multi-functionality. Hence, this paper describes a robot based on the most optimal possible in its field. The dynamic modeling of a flexible tail in the proposed robot are mentioned in detail. The robotic fish is composed of two links connected by an actuated joint; the frontal link is rigid and acts as the robotic fish body, while the rear link serves as the tail. The latter comprises a rigid element connected to a flexible caudal fin, whose underwater vibration is responsible for propulsion. The dynamics of the frontal link are described using Kirchhoff's equations of motion for rigid bodies in quiescent fluids. The tail vibration is modeled using Euler–Bernoulli beam Theory. Such methods could be a prospect approach for further research in the field of underwater robots.

Keywords: Micro-actuators, Biomimetic Fin, Bio-inspired Tail, Robot, Hydrodynamic Modeling, Drag Force, Lifting Force

1. Introduction

Some micro-robots have been developed to be a compact and multi-functionality structure with efficient and precise motion with inspiration from endoskeleton structures of varieties creature pattern locomotion [1, 2]. Every available systems for major scale mechanical machine (revolute and telescopic joints, motors and powerful structural members) become more to the following size reductions, since the surface effects commence to overcome over Newtonian forces [3].

For this reason, small scale systems based on traditional 'macro'-scale making techniques are articulated structures and morphologically limited using slithering or revolute surfaces would be deficient. A few primary bio-inspired structures have been attempted for micro-robotic mechanisms such as folded structures [4], micro-robotic confederacy [5], hinge joints [6] and prototype biomimetic micro-robots [7], [8]. Several types of existing smart materials technologies [9] are considered as candidates as artificial muscles in micro-robots [10,11]: pneumatic actuators, electromagnetic actuators, Electro-Active Polymers (EAPs), Ionic Polymer Metal Composite (IPMC) actuators [12], pneumatic actuators, Shape Memory Alloy (SMA) actuators [13], Ionic Conducting Polymer Film (ICPF) actuators [14,15] and piezoelectric elements. Recent studies researchers, with using of living creatures various underwater biomimetic robots have been developed, which consist of:

Qin Yan et al. proposed a flexible robotic fin by using SMA actuator [16]. Shiwu Zhang et al. designing and implementation of a lightweight bio-inspired Pectoral fin by SMA actuator was also reported [17]. Phi Luan Nguyen et al.

developed dynamic modeling of a non-uniform flexible tail for a robotic fish [18]. Dongwoo Lee et al. used SMA actuators in order to fabricate a biomimetic robotic jellyfish (Robojelly) [19]. Byungkyu Kim et al. Implementation of a biomimetic earthworm, which can be activated to mimic real locomotive mechanism for capsule endoscopes [20]. ICPF actuators are type of soft actuators which could be used in bio-inspire micro-robot, such as fish-inchworm underwater micro-robot.

We created posture amphibious to development the range of locomotion of the overall the micro-robot as shown in Figs 1, 2. The proposed body has both a compact structure and maximum interior space, compared to a streamlined body. It can rotate and change direction more easily than a streamlined design which is very important especially for micro-robots in pent up spaces.

In this paper, we designed and controlled the mechanical system of a novel type fish-inchworm micro-robot with eleven micro ICPF actuators, which used as legs. This unit employs seven of its micro actuators to walk, float and rotate. The other two micro actuators are utilized to implement grasping. Although the swimming [21] motion cannot guarantee than other motion patterns the position precision for the micro-robot. Hence, the fish- inchworm propulsion mechanisms just mimic the undulating and oscillatory body/fin locomotion.

Fig. 1. *Locomotion patterns of an inchworm. Climbing of leaf edges (upper right), Standing, (middle right), and Bending to change the direction (lower right).*

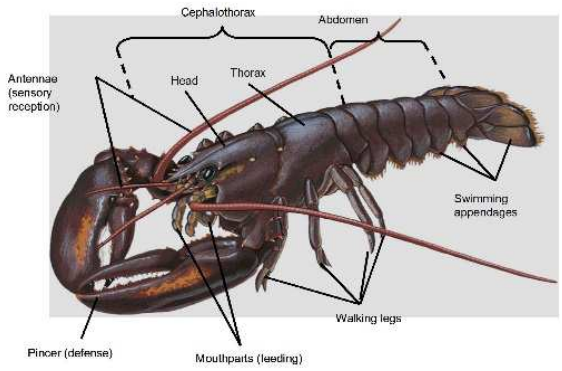

Fig. 2. *An anatomy mature of a H. gammarus.*

In addition, if compared with previous individual micro-robots, the system offers the following advantages:

1. According to the motional mechanism of biomimetic and because of using actuators the range of motions of the overall system is expanded.
2. Using of two species the motional mechanism of biomimetic by way of floating motions and inchworm cause the relatively high speed and endurance of the micro-robot, as can be seen in Fig.1.
3. Two actuators are used in the front section with simple locomotion tasks such as grasping and carrying objects to a desired position.

In order to implement more functions of the robot, an insect-inspired robot with four motion attitudes is proposed in this article. The robot uses eleven ICPF actuators for locomotion and underwater mission, and two SMA actuators for attitude change. The robot can change between four attitudes, longitudinal direction, traverse direction, standing structure, and flying motion.

And the rest of paper organized as follows:

Section 2 deeply proposes the hydrodynamic damping for marine vehicles which is mainly caused by potential damping, skin friction, wave drift damping, Vortex shedding damping, and viscous damping.

Section 3 states a dynamic modeling for a robotic fish, propelled by a tail with a flexible caudal fin. The design of a simple mechanical robotic fish is based on the animal behavior studies and outreach activities. The proposed nonlinear sixth-order model accounts for the interlaced relationship between propulsive forces induced by an undulating tail and the motion of the robot. In particular, the robot's dynamics, modeled using Kirchhoff's equations of motion, are coupled with the vibration of the undulating compliant fin, modeled using Euler–Bernoulli beam theory. The presence of the surrounding fluid is described through the use of hydrodynamic derivatives for the body and the Morison equation for both the peduncle and the fin. The fin motion-dependent thrust production is approximated from static thrust data, adapted from a previous work on a similar robot's propulsive system.

Section 4 establishes, the most important section, design and motion mechanisms of micro-robot. The features of proposed biomimetic robot, compared with previous papers, is both inchworm and fish in just one micro-robot without any contradiction, although it was a hard job. Mechanisms of both the walking and floating motion with and without payloads are simulated by MATLAB 2014b. Then a primary model for underwater robotics are performed by MATLAB 2014b. In order to reduce the elapsed time of simulation, the data are read from a worksheet on the Microsoft Excel spreadsheet (2013) and the numeric data are returned in an array by MATLAB. Finally, concluding remarks are presented.

Table 1. *List of Abbreviation.*

IPMC	Ionic Polymer Metal Composite
ICPF	Ionic Conducting Polymer Film
SMA	Shape Memory Alloy
DC	Direct Current
DOF	Degrees of Freedom

2. Hydrodynamic Damping

The hydrodynamic damping for marine vehicles is mainly caused by [22-25].

- potential damping
- skin friction
- wave drift damping
- vortex shedding damping
- viscous damping

The radiation-induced potential damping because of forced body oscillations is generally known as potential damping; its dynamic contribution is frequently slight with respect to, e.g., the viscous friction for under water vehicles while it may be significant for surface vessels. Linear skin friction is because of laminar boundary layers.

Wave drift damping is the dominant dynamic damping effect in surge motion of surface vessels in high sea. It can be supposed as an added resistance for boats advancing in waves. Its drift is proportional to the square of the significant wave height. In the sway and yaw directions, however, its dynamic contribution is negligible with respect to the effect of vortex shedding. When a body moves in a fluid it causes a separation of the flow. This can still be considered as laminar in the upstream while two anti-symmetric vortices can be observed in the downstream [26-30].

Vortex shedding is an unsteady flow which takes place at special flow velocities. In this flow vortices are created at the back of the body, periodically from each side. The viscosity of the fluid also causes dissipative forces.

These are composed of drag and lift forces, the former being parallel to the relative velocity of the vehicle with respect to the water while the latter are normal to it. The drag force could be modeled as [31-35]:

$$F_{\text{drag}} = \frac{1}{2}\rho\, U^2\, SC_{\text{d}}\,(R_n) \tag{1}$$

Where ρ is the fluid density, U is the velocity of the sphere, S is the frontal area of the body, C_d is the nondimensional drag coefficient, and R_n is the Reynolds number.For a generic body, S is the projection of the frontal area along the flow direction. The drag force can be considered as the sum of two physical effects: the frictional contribution of the surface whose normal is perpendicular to the flow velocity, and the pressure contribution of the surface whose normal is parallel to the flow velocity. For a hydrofoil moving in a fluid, the lift force can be modeled as [36-39]:

$$F_{\text{lift}} = \frac{1}{2}\rho\, U^2\, SC_1\,(R_n, \alpha) \tag{2}$$

Where S is the proposed area, C_1 is the nondimensional lift coefficient, and α is the angle of attack, i.e., the angle between the relative velocity and the tangent to the surface. For small angles of attack ($|\alpha| < 10^{\circ}$), the lift coefficient is proportional to α and quickly decays to zero as α increases [40].The drag and lift coefficients are therefore dependent on the Reynolds number, for instance on the laminar/turbulent fluid motion, as follows:

$$R_{\text{n}} = \frac{\rho|U|D}{\mu} \tag{3}$$

Where D is the characteristic dimension of the body perpendicular to the direction of U and μ is the dynamic viscosity of the fluid. Table 2 reports the drag coefficients as a function of the Reynolds number [41, 42].

Table 2. *Lift and drag coefficient.*

Reynolds number	Regime motion	C_{d}	C_{l}
$R_{\text{n}} < 2\times10^5$	Subcritical flow	1	3–0. 6
$2\times105 < R_{\text{n}} < 5\times10^5$	Critical flow	1–0. 4	0. 6
$5\times105 < R_{\text{n}} < 3\times10^5$	Transcritical flow	0. 4	0. 6

A common simplification considers only linear and quadratic damping terms and group these into a matrix D_{v} as follows:

$$D_{\text{v}}(\upsilon) > 0\,, \forall_{\upsilon}\, \epsilon \mathbb{R}^6 \tag{4}$$

3. Tail Dynamics

The robot's tail is connected to the body through an active hinge, physically corresponding to the servomotor shaft, located in the peduncle. The hinging point is at a distance from the body-fixed frame's origin O, along the negative - axis. The angle between the peduncle and the –axis

$$\emptyset(t) = Bsin(2\pi ft + \delta) + \overline{\emptyset}(t) \tag{5}$$

acts as the model's input parameter, through the angular amplitude , frequency , phase lag , and the robot's steering angle. The first summand in (5), corresponding to $\widetilde{\emptyset}(t)$ in Fig. 3, describes the periodic undulation of the peduncle about $\overline{\emptyset}(t)$. The steering angle $\overline{\emptyset}(t)$ can be kept constant, providing rectilinear or constant radius of curvature trajectories, or can be varied in time, at a rate typically smaller than a fraction of that of $\widetilde{\emptyset}(t)$ to allow for ample thrust generation during the maneuver, in order to accommodate more complex trajectories and maneuvers.

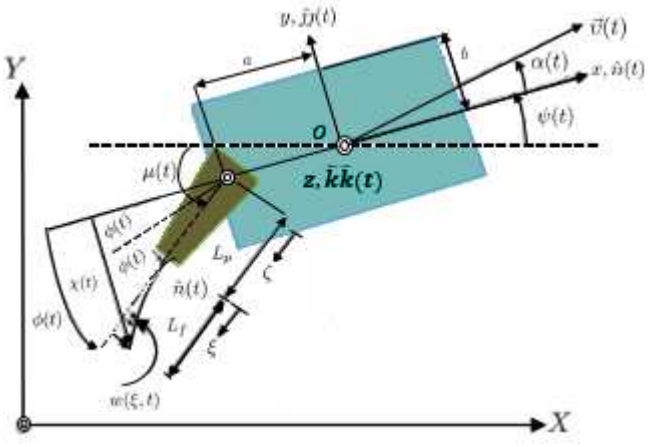

Fig. 3. *Schematic of in-plane swimming robotic fish, showing notation along with forces and moments acting on the body (inset).*

The peduncle and the fin are modeled as rigid and flexible beams, respectively. The rigid beam is connected to a translating hinge, and the flexible beam is cantilevered to it, as can be seen in Fig. 3. The fin has bending stiffness

$K_M(\xi) = (1/2)Eh^3\, d_f(\xi)$, where E is the Young modulus of the material, h is the fin's thickness, $d_f(\xi) = (2/5)\xi + 0.024$ is the length-dependent width of the fin, in meters, and is the material abscissa along the fin axis, ranging from 0 to L_f. Moreover, the proposed fin has a total area $A_f = \int_0^{L_f} d_f(\xi)d\xi$ and mass per unit length $\rho(\xi) = m_f d_f(\xi)/A_f$, with m_f=0.496× 10^{-3} kg being the total mass of the fin. Finally, the value of $Eh^3$is experimentally found to be 0.215 × 10^{-1} N m [43].

Regarding the reference [43], the elastic bending of the fin is described through the transverse displacement field $\omega(\xi, t)$, from the fin's undeformed configuration, demonstrated as the dash–dot–dot line in Fig. 3. It is worth noting that it is parallel to the unit vector $\hat{n}(t) = [\sin\mu(t)]\hat{l} - [\cos\mu(t)]\hat{\jmath}$, where $\mu(t) = \psi(t) + \phi(t)$. The procedure outlined in [43] permits for the description of the fin-tip displacement $q(t) = \omega(L_f, t)$ via a one-degree-of-freedom (1 DOF) modal model. The forced underwater vibration of the fin is described by the following partial differential equation (PDE) [43]:

$$[K_M(\xi)\omega''(\xi,t)]'' = F_f(\xi,t) - \rho(\xi)[\ddot{\vec{r}}_f(\xi,t).\hat{n}(t)] \quad (6)$$

where a prime denotes differentiation with respect to ξ and a dot denotes vector inner product. Equation (6) is complemented by boundary conditions consisting of clamping at the junction with the peduncle and a free-end condition at the tip of the fin [43]. In (6), $F_f(\xi, t)$ is the force per unit length due to the fluid–structure interaction, and also (ξ, t) is the acceleration of points on the fin. Both the body motion and the tail movement contribute to the absolute acceleration (ξ, t). By simple kinematics, we obtain

$$\ddot{\vec{r}}_f(\xi,t).\hat{n}(t) = \ddot{\vec{r}}_h(t).\hat{n}(t) + (L_P+\xi)\ddot{\mu}(t) + \ddot{\omega}(\xi,t) - \dot{\mu}^2(t)\omega(\xi,t) \quad (7)$$

where is the position of the hinge in the Earth-fixed frame, which can be computed from the location of the origin of the body-fixed frame. The fin is assumed to vibrate along its fundamental mode shape of in-vacuum vibrations $\Phi_1(\xi)$ for a trapezoidal beam geometry) and an approximate solution for the propulsor's motion is found using the classical Galerkin method; see, for example, [44]. Therefore, the displacement of points on the fin, with respect to the fin's undeformed configuration, is given by

$$\omega(\xi,t) = q(t)\Phi_1(\xi) \quad (8)$$

with $\Phi_1(L_f) = 1$. Consequently

$$\ddot{\vec{r}}_f(\xi,t).\hat{n}(t) = \ddot{\vec{r}}_h(t).\hat{n}(t) + (L_P+\xi)\ddot{\mu}(t) + \ddot{q}(t)\,\Phi_1(\omega) - \dot{\mu}^2(t)q(t)\Phi_1(\xi) \quad (9)$$

it can be inferred that the transverse acceleration of points on the fin accounts for the acceleration of the hinge point on the body $\ddot{\vec{r}}_h(t)$. The force per unit length acting on the fin due to the encompassing fluid is given by the Morison equation (see, for example, [45])

$$F_f(\xi,t) = -\tfrac{1}{2}\varrho(\dot{\vec{r}}_f(\xi,t).\hat{n}(t))\left|\ddot{\vec{r}}_f(\xi,t).\hat{n}(t)\right| d_f(\xi)C_{df} - \tfrac{1}{4}\pi\varrho\,(\ddot{\vec{r}}_f(\xi,t).\hat{n}(t))d_f^2(\xi)C_{df} \quad (10)$$

where C_{df} and C_{af} describe damping and added mass effects, including nonlinearities arising in moderately large amplitude oscillations [43-46]. The selection of values for these coefficients in the current work is obtained through curve fitting of the set of parameters in [43], available therein for undulatory frequencies of 1.0–2.0 Hz. The values of $C_{df} = 2.031$ and $C_{af} = 0.134$ are extrapolated from the fits for $f = 2.5$ Hz, which corresponds to the mean frequency of those investigated in this study. Further, the velocity of points along the fin is:

$$\dot{\vec{r}}_f(\xi,t) = \dot{\vec{r}}_p(L_P+\xi,t) + q\dot{(t)}\Phi_1(\xi)\hat{n}(t) + q(t)\Phi_1(\xi)\dot{\hat{n}}(t) \quad (11)$$

where the first summand is the rigid body motion imposed by the peduncle, which can be computed through simple kinematics. Combining (5) with (8) and (9), multiplying both sides of (5) by $\Phi_1(\xi)$, and integrating between 0 and L_f, the following modal model for the tail vibration is obtained:

$$\begin{aligned} M\ddot{q}(t) + P\sin\phi(t)\dot{u}(t) - P\cos\phi(t)\dot{v}(t) \\ + [Pa\cos\phi(t) + G]\dot{r}(t) \\ = \left[M_{\dot{\mu}^2}(t) - K\right]q(t) - G\ddot{\phi}(t) + R(t) \\ + P[u(t)r(t)\cos\phi(t) \\ + u(t)r(t)\sin\phi(t) \\ - ar^2(t)\sin\phi(t)] \end{aligned} \quad (12)$$

where M is the modal mass that accounts for both the fin dry mass and the added mass phenomenon. P and G are also associated with inertia effects, and are influenced by the rigid body motion of the fin. $R(t)$ is related to the hydrodynamic damping (see section 2). Remember that all of the parameters in (12) are known *a priori*. We remark that (12) cannot be independently solved for $q(t)$ in terms of the joint rotation$\phi(t)$, since the evolution of the fin-tip displacement $q(t)$ is related to the body motion. Therefore, an independent computation of the disturbance forces acting on the hinge, namely lift and moment, cannot be carried out. With reference to Fig. 3, those disturbances are as follows:

$$\mathcal{L}(t) = -m_p a_p(t) + V_f(t)\cos\phi(t) \quad (13a)$$

$$\mathrm{M}(t) = -Q(t) + M_f(t) - V_f(t)L_p + M_p(t) \quad (13b)$$

where

$$Q(t) = I_{p\ddot{\mu}}(t) + m_p L_{CGp}\left(\ddot{\vec{r}}_f(\xi,t).\hat{n}(t)\right) + m_p L_{CGP}^2\ddot{\mu}(t) \quad (14)$$

sncludes the rate of change of the angular momentum of the peduncle in respect to its center of mass and the moment of the linear momentum about the hinge. Here, is the mass of the peduncle and is equal to 1.70×10 kg, is the peduncle's mass moment of inertia about its center of mass and is equal to 2.72×10 kg m, both considering the presence of the servomotor, and $a_p(t) = \ddot{r}_p\ (L_{CGp}, t).\hat{\jmath}(t)$ is the component of the peduncle's center of mass' acceleration in the $\hat{\jmath}(t)$direction, located at a distance$L_{CGp} = 0.01$ m from the hinge and given by

$$\ddot{r}_p(L_{CGp}, t).\hat{\jmath}(t) = \dot{v}(t) + u(t)r(t) - a\dot{r}(t) - L_{CGp}\ddot{\mu}(t)\cos\phi\,(t) + L_{CGp}\dot{\mu}^2(t)\sin\phi\,(t) \quad (15)$$

While the first summands in (13a) and (13b) account for the peduncle's inertia, the latter terms describe the reaction shear force $V_f(t)$ and moment $M_f(t)$at the junction with the fin, along with the total force $F_p(t)$ and the total moment about the hinge $M_p(t)$acting on the peduncle by the fluid during the robot's motion.

The reactions at the junction are described as functions of the fin-tip displacement

$$V_f(t) = K_M(0)\Phi_1'''(0)q(t) \quad (16.a)$$

$$M_f(t) = K_M(0)\Phi_1''(0)q(t) \quad (16.b)$$

The Morison equation is also used to model the effect of the fluid on the peduncle, respectively, giving the total force and moment as

$$F_p(t) = \int_0^{L_p}\left(-\frac{1}{2}\varrho\left(\dot{r}_p\ (\zeta, t).\hat{n}(t)\right)\left|\dot{r}_p\ (\zeta, t).\hat{n}(t)\right| d_p(\zeta)C_{dp} - \frac{1}{4}\pi\varrho\left(\ddot{r}_p\ (\zeta, t).\hat{n}(t)d_p^2(\zeta)C_{ap}\right)d\zeta \quad (17.a)$$

$$M_p(t) = \int_0^{L_p}\left(-\frac{1}{2}\varrho\left(\dot{r}_p\ (\zeta, t).\hat{n}(t)\right)\left|\dot{r}_p\ (\zeta, t).\hat{n}(t)\right| d_p(\zeta)C_{dp} - \frac{1}{4}\pi\varrho\left(\ddot{r}_p\ (\zeta, t).\hat{n}(t)d_p^2(\zeta)C_{ap}\right)\zeta d\zeta \quad (17.b)$$

Where $d_p(\zeta) = 0.03 - (10/35)\zeta$ is the width along the peduncle, in meters, and $C_{dp} = 2.551$ and $C_{ap} = 1.479$ are, respectively, the damping and added mass coefficients for the peduncle. These values are obtained from [47] by selecting fixed values for the cross-section aspect ratio, the frequency parameter, and the local amplitude parameter (respectively, presented as α, β, and ϵ in [47]) corresponding to the width, height, and absolute amplitude of the peduncle at its midpoint for $f = 2.5$ Hz. The selection of parameters corresponding to this frequency aims to yield a set of terms suitable for all operating conditions in this study. Here, $\ddot{r}_p(\zeta, t).\hat{n}(t)$and $\dot{r}_p\ (\zeta, t).\hat{n}(t)$ are, respectively, the transverse velocity and acceleration of points on the moving peduncle. Combining (13)–(17) shows that lift and moment disturbances are dependent on the body motion and cannot be computed independently of the tail vibration.

4. The Mechanisms of the Proposed Micro-robot

Inchworm was introduced in detail in Section 1. In previous section mathematical study based on the tail of spiny tuna (Thunnus albacares) was obviously clarified. Since we should develop the micro-robots in order to do difficult multi-functionality, the underwater robot tuna-inchworm, which consists of inchworm, H. gammarus, fish and tail of tuna -inchworm, was obviously introduced.

The robot tuna-inchworm comprises of a (rigid) body made by plastic, eleven ICPF actuators, two plastic sheets, a tail fin, and two SMA actuators. With regard to the SMA actuators that are fixed in the plastic sheets, the attitude of the micro-robot can change between lying structure and standing structure, as can be seen in Fig.4.The body of the robot is 37mm long, 23mm high, and 21mm wide. The actuators phase of the micro-robot in standing mode is equal to 90°. The height of the proposed multifunctional tuna-inchworm is roughly 5mm while it is in lying mode. The size of the whole eleven actuators in this work are 17mm long, 4mm wide and 0.3mm thick.

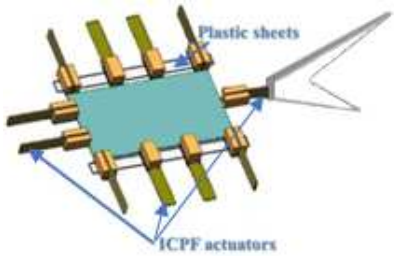

(a)

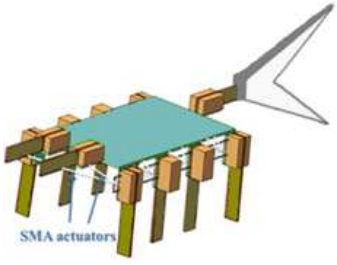

(b)

Fig. 4. (a) *Lying structure of the proposed micro-robot.****(b)*** *Standing structure of the proposed micro-robot.*

The purpose of using eleven micro actuators is for recognizing motion of micro-robot such as, walking, swimming, and rotating motions. The order of the eleven ICPF, with one DOF, actuators can be seen in Fig.5. In lying structure, actuators I and J are named fingers, which are used for grasping tiny objects, and actuators B, C, F, G and actuators A, D, E, H , which are named supporters and drivers separately, respectively used for locomotion of the micro-robot. But, in standing structure, actuators B, C, F, and G are named fingers for grasping motion, and actuators A, D, E, and H are also named drivers which are used for both walking and rotating motion. Finally, actuator K is named tail fin for swimming motion in both structures.

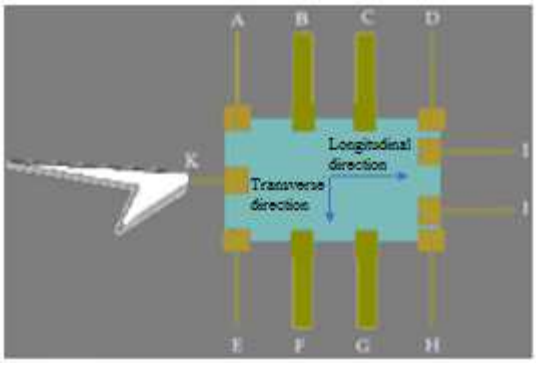

Fig. 5. *The Order of the eleven ICPF actuators (top).*

4.1. Mechanism of the Walking Motion

The walking mechanism of inchworm with one DOF can be seen in Fig.6. Based on the situation one leg is known as the leading legs, and the other one as the following legs. So, if the robot is walking in transverse direction, the leading and following legs are the same as what is seen Fig.4.b, otherwise the leading and following legs change so as to get to the longitudinal direction. In order to analyze the walking motion of inchworm carefully, its motion is divided into five periods (See Fig.6 letters a to e). Fig.6 also clarifies that the robot moves a distance of 2*d* during a single pace cycle.

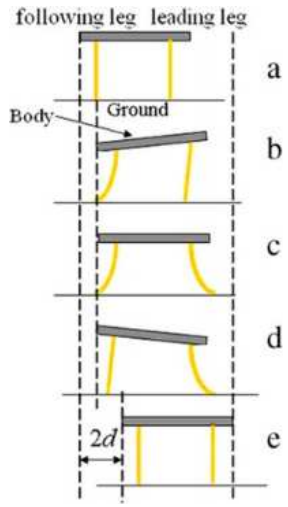

Fig. 6. *Micro-robot crawling mechanism [48, 58]*

In order to simulate the speed of walking motion of the proposed robot, the displacement of the drivers and the input frequency are considered. Note that the displacement of the actuator in an actual application is demonstrated by d the actuator, and also the displacement of the actuator without payload is demonstrated by d_0. Regarding the water resistance, potential damping, vortex shedding damping, viscosity, payload, and other factors, the displacement of the drivers decreases by a non-negligible amount $1d$. Hence, the relationship between d_0 and d and the walking speed of the micro-robot are as follows [48-51]:

$$d = d_0 - \Delta d \tag{18}$$

$$v = 2f(d_0 - \Delta d) \tag{19}$$

where v is the average speed and f is the frequency of the input signal. Note that the average speed depends on the input frequency obtained from the average of experimental or theoretical results.

4.2. Mechanism of the Rotating Motion

As can be seen in Fig.5 the two legs A, and D are used as following legs and legs B, and C as leading legs. This simple movement makes the micro-robot easily to rotate clockwise. Now, if the leading and the following legs change, the counter-clockwise rotation is considered. The speed of the rotating motion can be simply calculated by the rotational angle covered in a single cycle and the frequency of the pace [52-56].

The displacement of a single ICPF actuator by applying different signals is carefully calculated in order to simulate the theoretical walking/crawling speed of the robot. The theoretical displacements d_0, without payload, of the actuator can be seen in Fig.7. The simulation results of the theoretical walking speed can be clearly seen in Fig 8. Regarding the simulation results, it is concluded that if the frequency increases, the dispalcements of ten actuators increase. this is good because the proposed micro-robot has a maxiumam walking speed. If the response from the displacements of actuators don't last, it will help us to develop a faster biomimeric micro-robot in future. Fast response is too important in micro-robots and also in nano-robots.

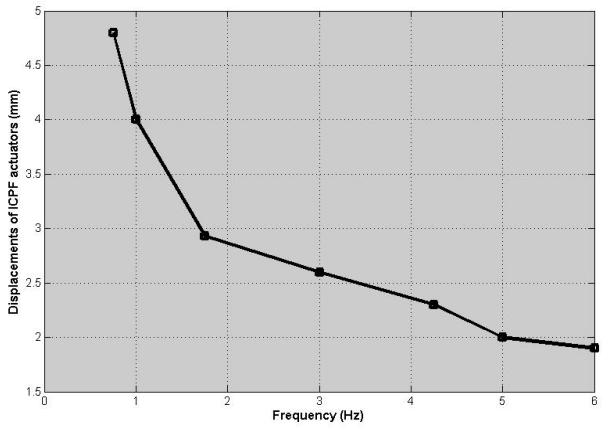

Fig. 7. *The displacement (d_0) of the ICPF actuator (7 V).*

4.3. Grasping and Floating Simulations with and without Payloads

Fig.9 shows the simulation of floating speeds with and without payloads. The maximum speed while grasping a 0.5 g object tends to 4.73 mm/s. The maximum payload which the micro-robot is able to float upward is 0.6 g. As can be seen, all curves decrease if the frequency is higher than 0.1 Hz.

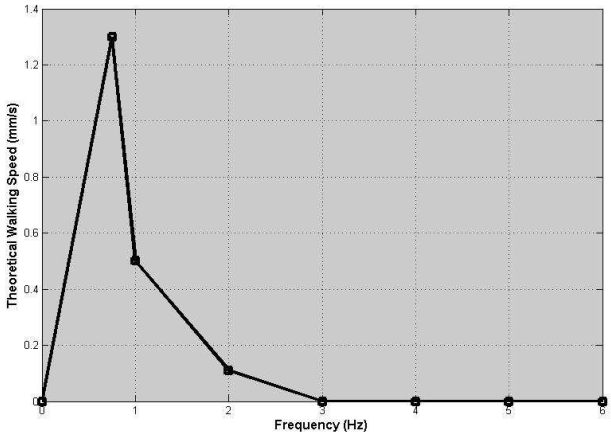

Fig. 8. *Theoretical walking speed of the Micro-robot (7 V).*

4.4. Simple Algorithm for Obstacle Avoidance

As a matter of fact developing underwater micro-robot without considering obstacles is so useless. In this work inchworm-jellyfish is proposed to do simple mechanisms such as floating, rotating, walking, and moreover lying mode. These mechanisms help the proposed robot so as to bypass the obstacles. So ultrasonic sensor (AVR-ATMEGA 32) is chosen.

Ultrasonic sensors, which are mounted on the proposed robot body, detect the distance robot and the objects which are close to it. The processor measures the time interval between the sent signals from the reflected back according to the robot speed and distance to the obstacle, therefore the robot bypass and take the safe route.

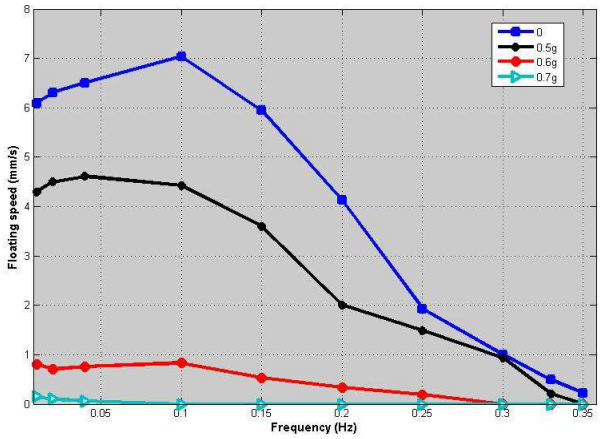

Fig. 9. *Theoretical floating speed results with and without payloads (7V).*

5. Conclusions and Future Works

In this work, a novel underwater micro-robot was with a compact, multi-functional, and flexible structure obtained using eleven ICPF actuators as biomimetic legs or fingers was introduced. This robot is combination of three creatures such as tuna, inchworm, gammarus. The inchworm mechanism is used in walking motion and gammarus as a grasping (fingers), and finally tuna tail for this research. Though it was a hard job. An unsteady, multi-block overset grid and set of complex and differential equation has been developed in order to numerically investigate the self-propelled motion of a fish with a pair of pectoral fins which would be legs in walking motion in this research.

The dynamic modeling of a flexible tail in the proposed micro-robot are mentioned in detail. Parameters such as $\dot{\vec{r}}_p(\zeta,t).\hat{n}(t)$ and $\ddot{\vec{r}}_p(\zeta,t).\hat{n}(t)$ are the transverse velocity and acceleration of points on the moving peduncle. Combining equations 13-17 shows that lift and moment disturbances are dependent on the body motion and cannot be computed independently of the tail vibration and can be a prospect approach for further research in the field of underwater micro-robot.

As the future work in this field, the mechanical structure and also the navigation will be designed to be intelligent. In order to aim this, meta-heuristic methods such as genetic algorithms are very helpful. To evaluate the performance of mechanical structure design in different environments modeling of a robot navigation environment is used and then make some different scenarios in order to estimate the performance of mechanical structure. Given that the study of mechanical and structure properties in different environments require intelligent methods, so the genetic algorithms can be used to get the best structure depending on the characteristics of the different navigation. To check the routing path according to the characteristics of the design robot, the processor can be programmed using meta-heuristic methods to improve its performance.

But, there are still some obstacles and problems which must be studied in the future as follows:

1. Using the materials which can effectively mimic jellyfish movement except IPMC and ICPF actuators.
2. Improving the transportation over the amount offered in this paper.
3. Designing micro-robot with this size or smaller than the amount offered for more depth.

Appendix

1. Simulation for floating of Micro-robot with and without payload (MATLAB 2014b, Win-64) [57, 58].

```
function [condition]=floating
format short;
disp(pwd);          % displays the MATLAB® current folder.
```

```
   disp(computer);   % Information about computer on which MATLAB® software is running.
   disp(license);    %Return license number or perform licensing task.
   display('------------------------------------------------------------');
   tic;
   %
   g=9.8066;  % gravitational acceleration.
   Density =input('Enter the density of your experiment= ');
   deltav=0;     %usually considered to be zero in the calculations.
   m=input('Enter the mass of robot (kg)= ');
   disp(' ');  %Insert a blank line.
   v=input('Enter the volume of robot(m^3)= ');
   disp('  ');     %Insert a blank line.
   %
   Condition=(Density)*g*(v+deltav))
   display('Please wait...');
   %
   %
   display('The simulation result is:');
   if Condition = (m*g)
      display('*****suspended*****');
   else if Condition >(m*g)
         display('*****floating upward*****');
      else
         display('*****sinking downward*****');
      end;
   end;
   toc;
   workspace;
   disp(date);  % This MATLAB® function returns a string containing the date in dd-mmm-yyyy format.
```

References

[1] Liwei Shi, Shuxiang Guo, Shaowu Pan, Yanlin He, Ping Guo, A Multifunctional Underwater Microrobot for Mother-Son Underwater Robot System, Proceeding of the IEEE International Conference on Robotics and Biomimetics (ROBIO) Shenzhen, China, December 2013.

[2] Choi, Hyunchul, Semi Jeong, Cheong Lee, Gwangjun Go, Kiduk Kwon, Seong Young Ko, Jong-Oh Park, and Sukho Park. "Biomimetic swimming tadpole microrobot using 3-pairs Helmholtz coils." In Biomedical Robotics and Biomechatronics (2014 5th IEEE RAS & EMBS International Conference on, pp. 841-844. IEEE, 2014.

[3] W.S.N. Trimmer. Microrobots and micromechanical systems. J. of Sensors and Actuators, 19:267–287, 1989.

[4] R. Yeh, E.J.J. Kruglick, and K.S.J. Pister. Surface-micromachined components for articulated microrobots. J. of Microelectrical Mechanical Systems, 5(1):10–17, March 1996.

[5] R. Yeh, S. Hollar, and K.S.J. Pister. Design of low-power silicon articulated microrobots. J. of Micromechatronics, 1(3):191–203, 2002.

[6] K.S.J. Pister, M.W. Judy, S.R. Burgett, and R.S. Fearing. Microfabricated hinges. J. of Sensors and Actuators A: Physical, 33:249–256, 1992.

[7] S. Hollar, A. Flynn, C. Bellew, and K.S.J. Pister. Solar powered 10mg silicon robot. In MEMS, Kyoto, Japan, January 2003.

[8] T. Ebefors, J.U. Mattsson, E. K¨alvesten, and G. Stemme. A walking silicon micro-robot. In The 10th Int. Conf. on Solid-State Sensors and Actuators (Transducers '99), pages 1202–1205, Sendai, Japan, June 1999.

[9] Isidro Cobo, Ming Li, Brent S. Sumerlin and Sébastien Perrier, Smart hybrid materials by conjugation of responsive polymers to biomacromolecules, Nature Materials 14, 143–159 (2015).

[10] Nguyen Kim Tien, Doyeon Hwang, Sunyong Jung, Seong Young Ko, Jong-Oh Park, and Sukho Park, Development of Bio-inspired Walking micro-robot using PVDF/PVP/PSSA-based IPMC Actuator, Proceedings of 2014 IEEE International Conference on Mechatronics and Automation August 3 - 6, Tianjin, China.

[11] Yuen Kuan Yong, and Andrew J. Fleming, Piezoelectric Actuators with Integrated High-Voltage Power Electronics, IEEE/ASME TRANSACTIONS ON MECHATRONICS, VOL. 20, NO. 2, APRIL 2015 pp. 611-617.

[12] Siul Ruiz, Benjamin Mead, Viljar Palmre, Kwang J Kim and Woosoon Yim, A cylindrical ionic polymer-metal composite based robotic catheter platform: modeling, design and control, Smart Mater. Struct. 24 (2015) 015007 (11pp).

[13] Jaronie Mohd Jani , Martin Leary , Aleksandar Subic , Mark A. Gibson, A review of shape memory alloy research, applications and opportunities, Materials and Design 56 (2014) 1078–1113.

[14] Shuxiang Guo, Fu Wan, Wei Wei, Jian Guo,Yunliang Wang, An Underwater Microrobot with Six Legs Using ICPF Actuators, Proceedings of 2013 ICME International Conference on Complex Medical Engineering May 25-28, Beijing, China.

[15] Wei Wei, Fu Wan, Nan Liu, Yao Lu, Bang Yang, A Novel Water-drop Power Generation System Based on ICPF Actuator, Proceeding of the IEEE International Conference on Robotics and Biomimetics (ROBIO) Shenzhen, China, December 6 (2013)1001-1006.

[16] Qin Yan, Lei Wang, Bo Liu, Jie Yang, Shiwu Zhang, A Novel Implementation of a Flexible Robotic Fin Actuated by Shape Memory Alloy, Journal of Bionic Engineering 9 (2012) 156–165.

[17] Shiwu Zhang, Bo Liu, Lei Wang, Qin Yan, Kin Huat Low, and Jie Yang, Design and Implementation of a Lightweight Bioinspired Pectoral Fin Driven by SMA, IEEE/ASME TRANSACTIONS ON MECHATRONICS, VOL. 19, NO. 6, DECEMBER 2014.

[18] Phi Luan Nguyen, Van Phu Do, Byung Ryong Lee, Dynamic Modeling of a Non-Uniform Flexible Tail for a Robotic Fish, Journal of Bionic Engineering 10 (2013) 201–209.

[19] Alex Villanueva, Colin Smith and Shashank Priya, A biomimetic robotic jellyfish (Robojelly) actuated by shape memory alloy composite actuators, Bioinsp. Biomim. 6 (2011) 036004 (16pp).

[20] Kim, Byungkyu, Sukho Park, Chang Yeol Jee, and Seok-Jin Yoon. "An earthworm-like locomotive mechanism for capsule endoscopes." In *Intelligent Robots and Systems, 2005.(IROS 2005). 2005 IEEE/RSJ International Conference on*, pp. 2997-3002. IEEE, 2005.

[21] Alessandro Crespi • Daisy Lachat • Ariane Pasquier • Auke Jan Ijspeert, Controlling swimming and crawling in a fish robot using a central pattern generator, Auton Robot (2008) 25: 3–13.

[22] S. Guo, L. Shi, K. Asaka, and L. Li, "Experiments and Characteristics Analysis of a Bio-inspired Underwater micro-robot", Proceeding of the 2009 IEEE International Conference on Mechatronics and Automation, pp.3330-3335, Changchun, China, August 9-12, 2009.

[23] Hyunchul Choi, Gwangjun Go, Cheong Lee, Seong Young Ko, Semi Jeong, Kiduk Kwon, Jong-Oh Park and Sukho Park, Member, IEEE, Electromagnetic Actuation System for Locomotive Intravascular Therapeutic micro-robot, 2014 5th IEEE RAS & EMBS International Conference on Biomedical Robotics and Biomechatronics (BioRob) August 12-15, 2014. São Paulo, Brazil.

[24] Takuya Okada, Shuxiang Guo, Fu Qiang and Yasuhiro Yamauchi, A Wireless micro-robot with Two Motions for Medical Applications, Proceedings of the 2012 ICME International Conference on Complex Medical Engineering July 1 - 4, Kobe, Japan.

[25] Je-Sung Koh, and Kyu-Jin Cho, Omega-Shaped Inchworm-Inspired Crawling Robot with Large-Index-and-Pitch (LIP) SMA Spring Actuators, IEEE/ASME TRANSACTIONS ON MECHATRONICS, VOL. 18, NO. 2, APRIL 2013, pp.419-429.

[26] Lye`s Mellal, Karim Belharet, David Folio, Antoine Ferreira, Optimal structure of particles-based superparamagnetic microrobots: application to MRI guided targeted drug therapy, J Nanopart Res (2015) 17:64.

[27] Bu Hyun Shin, Kyung-Min Lee, Seung-Yop Lee, A Miniaturized Tadpole Robot Using an Electromagnetic Oscillatory Actuator, Journal of Bionic Engineering 12 (2015) 29–36.

[28] B. Behkam, and M. Sitti, "Design methodology for biomimetic propulsion of miniature swimming robots," Journal of Dynamic Systems, Measurement, and Control, Vol.128, No. 1, pp. 36-43, 2006.

[29] W. Zhang, S. Guo and K. Asaka, "A New Type of Hybrid Fish-like micro-robot", International Journal of Automation and Computing, Vol.3, No.4, pp. 358-365, 2006.

[30] Isidro Cobo, Ming Li, Brent S. Sumerlin and Sébastien Perrier, Smart hybrid materials by conjugation of responsive polymers to biomacromolecules, Nature Materials 14, 143–159 (2015).

[31] Siul Ruiz, Benjamin Mead, Viljar Palmre, Kwang J Kim and Woosoon Yim, A cylindrical ionic polymer-metal composite based robotic catheter platform: modeling, design and control, Smart Mater. Struct. 24 (2015) 015007 (11pp).

[32] Shuxiang Guo, Fu Wan, Wei Wei, Jian Guo, Yunliang Wang, An Underwater Microrobot with Six Legs Using ICPF Actuators, Proceedings of 2013 ICME International Conference on Complex Medical Engineering May 25-28, Beijing, China.

[33] Wei Wei, Fu Wan, Nan Liu, Yao Lu, Bang Yang, A Novel Water-drop Power Generation System Based on ICPF Actuator, Proceeding of the IEEE International Conference on Robotics and Biomimetics (ROBIO) Shenzhen, China, December 6 (2013)1001-1006.

[34] Nguyen Kim Tien, Doyeon Hwang, Sunyong Jung, Seong Young Ko, Jong-Oh Park, and Sukho Park, Development of Bio-inspired Walking micro-robot using PVDF/PVP/PSSA-based IPMC Actuator, Proceedings of 2014 IEEE International Conference on Mechatronics and Automation August 3 - 6, Tianjin, China.

[35] Yuen Kuan Yong, and Andrew J. Fleming, Piezoelectric Actuators with Integrated High-Voltage Power Electronics, IEEE/ASME TRANSACTIONS ON MECHATRONICS, VOL. 20, NO. 2, APRIL 2015 pp. 611-617.

[36] Jenhwa Guo, Maneuvering and control of a biomimetic autonomous underwater vehicle, Auton Robot (2009) 26: 241–249.

[37] Yuh, Junku. "Design and control of autonomous underwater robots: A survey." Autonomous Robots 8, no. 1 (2000): 7-24.

[38] Şafak, Koray K., and George G. Adams. "Dynamic modeling and hydrodynamic performance of biomimetic underwater robot locomotion." Autonomous Robots 13, no. 3 (2002): 223-240.

[39] B. Kim, M.G. Lee, Y.P. Lee, Y. Kim, G. Lee, An earthworm-like micro robot using shape memory alloy actuator, Sensors and Actuators A: Physical 125 (2) (2006) 429–437.

[40] S. Liu, T. Huang, J. Yen, Comparison of sensor fusion methods for an SMA-based hexapod biomimetic robot, Robotics and Autonomous Systems 58 (5) (2010) 737–744.

[41] A. Hadi, A. Yousefi-Koma, M.M. Moghaddam, M. Elahinia, A. Ghazavi, Developing a novel SMA-actuated robotic module, Sensors and Actuators A: Physical 162 (1) (2010) 72–81.

[42] M. Shahinpoor, K.J. Kim, Ionic polymer-metal composites: IV. Industrial and medical applications, Journal of Smart Materials and Structures 14 (2005) 197–214.

[43] V. Kopman and M. Porfiri, "Design, modeling, and characterization of a miniature robotic-fish for research and education in biomimetics and bioinspiration," *IEEE/ASME Trans. Mechatron.*, vol. 18, no. 2, pp. 471–483, Apr. 2013.

[44] R. C. Batra, M. Porfiri, and D. Spinello, "Electromechanical model of electrically actuated narrow microbeams," *J. Microelectromech. Syst.*, vol. 15, no. 5, pp. 1175–1189, Oct. 2006.

[45] J. M. J. Journée and W.W.Massie, Offshore Hydromechanics. Delft, The Netherlands: Delft University of Technology, 2001, ch. 12.

[46] J. M. R. Graham, "The forces on sharp-edged cylinders in oscillatory flow at low Keulegan-Carpenter numbers," *J. Fluid Mech.*, vol. 91, no. 2, pp. 331–346, 1980.

[47] C. N. Phan, M. Aureli, and M. Porfiri, "Finite amplitude vibrations of cantilevers of rectangular cross sections in viscous fluids," *J. Fluids Struct.*, vol. 40, pp. 52–69, 2013.

[48] http://www.nationallobsterhatchery.co.uk/whats-it-all-about/education/lobster-biology

[49] J.C. Kinsey, R.M. Eustice, L.L. Whitcomb: A survey of underwater vehicle navigation: recent advances and new challenges, 7th IFAC Conf. Manoeuvring Contr. Marine Craft (IFAC, Lisbon 2006).

[50] D.A. Smallwood, L.L. Whitcomb: Adaptive identification of dynamically positioned underwater robotic vehicles, IEEE Trans. Contr. Syst. Technol. 11(4), 505–515 (2003).

[51] O.M. Faltinsen: Sea Loads on Ships and Offshore Structures (Cambridge University Press, Cambridge 1990).

[52] Alvarado P V, Youcef-Toumi K. Design of machines with compliant bodies for biomimetic locomotion in liquid environments. *Journal of Dynamic Systems, Measurement, and Control*, 2006. 128, 3–13.

[53] Suppiger E W, Taleb N J. Free lateral vibration of beams of variable cross section. *Zeitschrift für Angewandte Mathematik und Physik* (*ZAMP*), 1956, 7, 501–520.

[54] Phi Luan Nguyen, Van Phu Do, Byung Ryong Lee*, Dynamic Modeling of a Non-Uniform Flexible Tail for a Robotic Fish, Journal of Bionic Engineering 10 (2013) 201–209.*

[55] S. Zhao, J. Yuh: Experimental study on advanced underwater robot control, IEEE Trans. Robot. 21(4), 695–703 (2005).

[56] El Daou H, Salumae T, Toming G, Kruusmaa M. A bio-inspired compliant robotic fish: Design and experiments. *The 2012 IEEE International Conference on Robotics and Automation*, Saint Paul, MN, USA, 2012, 5340–5345.

[57] Alvarado P V. *Design of Biomimetic Compliant Devices for Locomotion in Liquid Environments*, PhD Thesis, Massachusetts Institute of Technology, Cambridge, USA, 2007.

[58] Alireza Shourangiz Haghighi, Amin Haghnegahdar, Reza Jahromi Bosheri, Iman Zare. Micro-embedded Skimmer in Autonomous Underwater Micro-robots. *International Journal of Science and Qualitative Analysis*. Vol. 1, No. 3, 2015, pp. 43-53.